JOC The Journal of Organic Chemistry

Article

pubs.acs.org/joc

Origins of Stereoselectivity of Enamine−Iminium-Activated Nazarov Cyclizations by Vicinal Diamines

Adam Simon, Yu-hong Lam, and K. N. Houk*

Department of Chemistry and Biochemistry, University of California, Los Angeles, California 90095-1569, United States

Supporting Information

ABSTRACT: The mechanism and sources of asymmetric induction in Nazarov reactions reported by Tius and co-workers have been determined with quantum chemical calculations. A chiral vicinal diamine forms an enamine−iminium adduct with α-ketoenones, and this undergoes a cationic conrotatory electrocyclization. The chiral diamine imparts stereocontrol in the enamine−iminium complex by forming a six-membered ring that favors one helicity of the electrocyclization transition state.

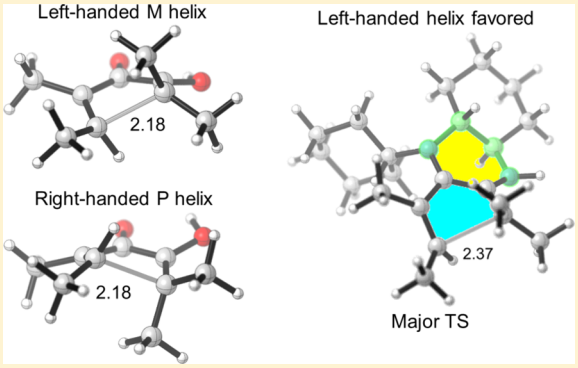

INTRODUCTION

Nazarov cyclizations are synthetically important reactions that generate cyclopentenones via a cationic 4π electrocyclization of a protonated dienone; up to three new contiguous carbon stereocenters can be generated in this reaction.[1] Nazarov reactions have achieved high levels of stereoselectivity by chiral Lewis acid catalysts,[2] chiral auxiliaries,[3] and recently organocatalysts.[4] Vicinal diamines are successful organocatalysts, because of their bifunctional and tunable behavior.[5] Tius reported that simultaneous enamine and iminium activation by a chiral vicinal diamine for stereoselective Nazarov reactions of α-ketoenones gave 11−63% yield and 90:10 to >99:1 enantiomeric ratios (Scheme 1).[6]

Computational modeling of stereoselectivity has been accomplished for many Nazarov reactions.[7,8] The first stereochemical model for an organocatalyzed Nazarov reaction was recently reported by our group.[8] These computational results explained the induction of asymmetry by a thiourea−primary amine catalyst,[4b] which favored one helical conformation in the Nazarov cyclization transition state. In the thiourea system, the electrocyclization occurred via an enol intermediate with hydrogen-bonding catalysis by the thiourea−primary amine. Enamine formation was unlikely due to the nonpolar conditions of the reaction. By contrast, the mechanism and source of stereoselectivity, as well as the cause of product inhibition in the diamine-mediated Nazarov reaction by Tius has not been studied computationally.[6] Tius proposed a simultaneous enamine−iminium intermediate that undergoes cyclization. We used density functional theory calculations to predict transition states for three pathways: two combinations of enamine−iminium activation at the two carbonyls, and an enamine intermediate that undergoes a Michael addition. The thermodynamics of the intermediates along the reaction coordinate were calculated to determine the source of product inhibition. The factors that control stereoselectivity, as well as a stereochemical model, are proposed.

Scheme 1. Chiral Diamine-Mediated Nazarov Cyclizations[6]

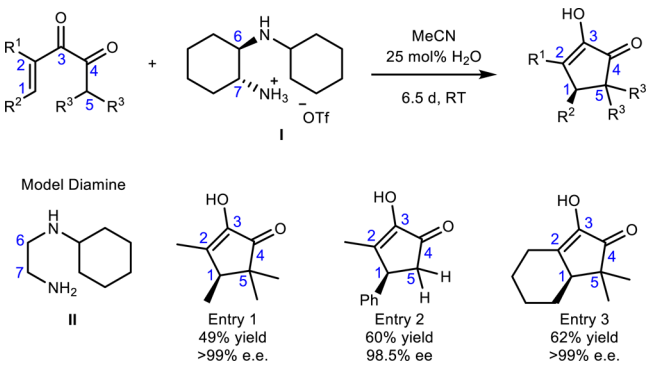

COMPUTATIONAL METHODS

The quantum chemical calculations were performed with Gaussian 09.[9] The geometries were fully optimized at the B3LYP[10]/6-31G(d) level of theory in conjunction with the IEF-PCM implicit solvation model[11] to account for solvation effects of acetonitrile (MeCN), the solvent used experimentally. All optimized geometries were verified by frequency computations as minima (zero imaginary frequencies) or transition structures (a single imaginary frequency). Free energy corrections were calculated using Truhlar's quasiharmonic approximation.[12] Free energies were obtained by performing single-point energy calculations on the optimized geometries with the density

Received: June 28, 2017
Published: July 5, 2017

DOI: 10.1021/acs.joc.7b01606
J. Org. Chem. 2017, 82, 8186−8190

functional method M06-2X[13]/def2-TZVPP[14] with the IEF-PCM model (MeCN). We found that the M06-2X/def2-TZVPP–IEF-PCM//B3LYP/6-31G(d)–IEF-PCM level of theory provides accurate geometries and energies, while being relatively efficient in computational times.[15] The lowest-energy transition structures were also optimized at the M06-2X/6-31G(d,p) level of theory in conjunction with single-point energies calculated using various dispersion-inclusive DFT methods. These methods qualitatively agree with the experimental results and are discussed in Supporting Information (SI).

RESULTS AND DISCUSSION

The reaction proceeds experimentally by exposing the α-ketoenone substrate to a full equivalent of diamine salt **I** in wet acetonitrile at room temperature for 6–7 days.[6] An unidentified intermediate forms containing the product. Acidic workup liberates the cyclopentenone from the intermediate with extremely high optical purity and modest yields. The free energy profile of the Nazarov cyclization involving **1** and diamine salt **I** (entry 1, Scheme 1) was calculated with the M06-2x/def2-TZVPP–IEF-PCM//B3LYP/6-31G(d)–IEF-PCM(MeCN) level of theory (Scheme 2). We predict the

Scheme 2. Proposed Mechanism of the Nazarov Reaction

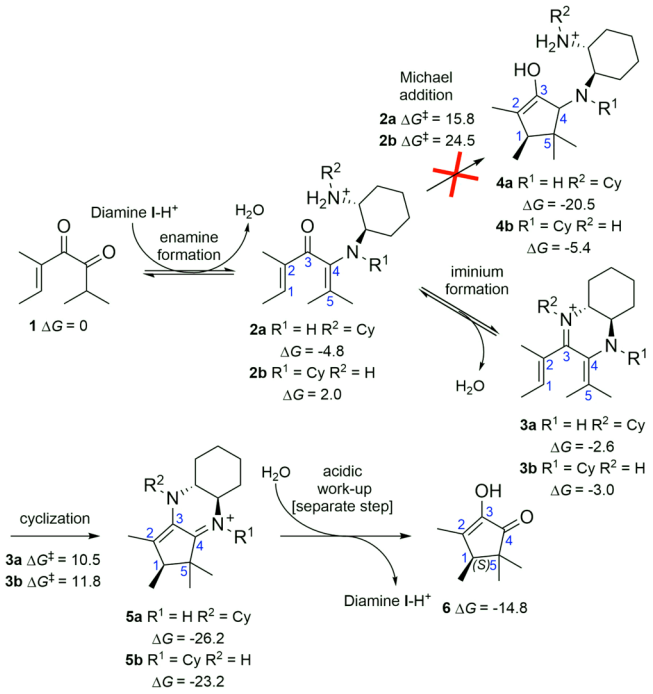

diamine forms an enamine at C4, which is the electrophilic carbonyl, to form **2a** or **2b**. Either the primary or the secondary amine can react at this position. The primary amine as the enamine nitrogen in **2a** is more stable by 6.8 kcal/mol because the cyclohexyl group is far from the methyl groups of the α-ketoenone. Enamine **2** can either undergo a Michael addition to form the product directly or proceed to the enamine–iminium intermediate **3**. The predicted barrier for the Michael addition is 15.8 kcal/mol for **2a** and 24.5 kcal/mol for **2b**. The Michael addition transition structures are illustrated and discussed in SI (Figure S1). The equilibrium formation of the intermediate **3** should occur readily, although we did not compute barriers for this equilibrium, which involve a number of proton shuffling processes with water. The enamine–iminium intermediate **3** is more stable than reactants by 2.6 and 3.0 kcal/mol for **3a** and **3b**, respectively. Either **3a** or **3b** reacts via the 4π electrocyclization with a barrier of only 10.5 kcal/mol for **3a** and 11.8 kcal/mol for **3b**. We predict that the electrocyclization mechanism is significantly lower in energy than the Michael addition mechanism and is the dominant pathway. The electrocyclization forms the highly stable enamine–iminium products **5a** and **5b**, which are 26.2 and 23.2 kcal/mol lower in energy than separated **1** and diamine **I**-H$^+$, respectively. The hydrolysis product **6** is 14.8 kcal/mol lower in energy. This agrees with the observed product inhibition when diamine **I** is used in substoichiometric quantities. Intermediate **5** requires acidic workup to release **6** via hydrolysis.

The electrocyclization transition state determines the stereochemistry. Entry 1, as reported by Tius, yields electrocyclization product **6** with (*S*) configuration at the newly formed chiral center with greater than 99% enantiomeric excess. We predict that diamine **I** forms the enamine with substrate **1** to give the enamine–iminium **3a** as the reactive complex; the primary amine first attacks the carbonyl of **1**. The lowest-energy transition structures for the electrocyclization of **3a** are shown in Figure 1.

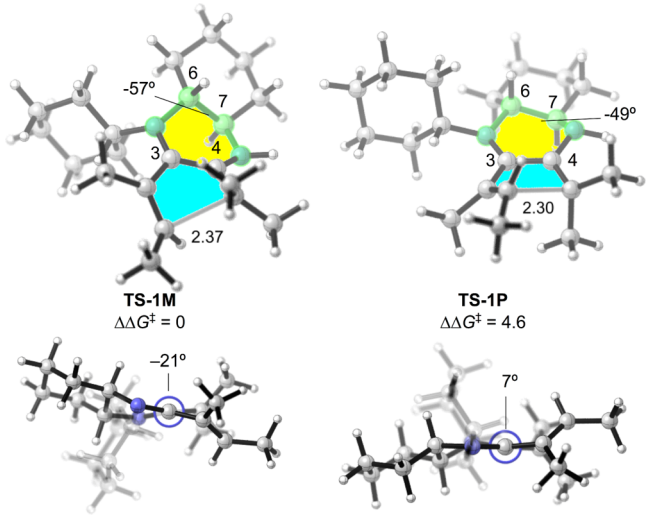

Figure 1. Lowest-energy transition structures for the Nazarov cyclization of the enamine–iminium intermediate **3a** derived from substrate **1** and diamine **I** leading to the major (*S*) and minor (*R*) products (M06-2X/def2-TZVPP–IEF-PCM//B3LYP/6-31G(d)–IEF-PCM (MeCN). Newman projections through C3 and C4 are shown below **TS-1M** and **TS-1P**. The cyclohexyl rings are transparent in the Newman projections for clarity. The relative free energies of activation compared with **TS-1M** are reported in kcal/mol.

The transition structure **TS-1M** leads to the major (*S*)-product. **TS-1P** yields the unobserved minor (*R*)-product and is higher in energy by 4.6 kcal/mol. The **M** and **P** (left- and right-handed helicity, respectively) in the **TS** series refer to the helical chirality of the forming five-membered ring that is highlighted in blue. The higher-energy transition structures are discussed in SI (Figure S2). The differences from those in Figure 1 are the disposition and conformations of the cyclohexyl ring and the conformations of the two six-membered rings. The difference in activation barriers between **TS-1M** and **TS-1P** ($\Delta\Delta G^{\ddagger}$ = 4.6 kcal/mol) agrees with the experimentally observed enantioselectivity (>99.5% ee (*S*), $\Delta\Delta G^{\ddagger}$ > 3.6 kcal/mol).

DOI: 10.1021/acs.joc.7b01606
J. Org. Chem. 2017, 82, 8186–8190

The stereocontrolling factor that differs between **TS-1M** and **TS-1P** is the helical chirality of the forming five-membered ring. The internal six-membered ring, highlighted in yellow, resembles a half-chair conformation in the transition structures. It is fused to an additional chair six-membered ring and resembles a *trans*-decalin. The N−C6−C7−N dihedral angle is −57° in **TS-1M** and −49° in **TS-1P**. Also shown in Figure 1 are Newman projections through C3 and C4 of the transition structures. The dihedral angle N−C3−C4−N is −21° in **TS-1M**, and 7° in **TS-1P**. **TS-1P** is more planar than **TS-1M**.

To understand what causes the difference in energy between transition structures **TS-1M** and **TS-1P**, a model system was studied with the external six-membered ring removed. This allows free rotation of the diamine and removes the chirality of C6 and C7. Computations of the enamine−iminium intermediate formed by **1** with achiral diamine **II** (Scheme 1) were performed. They reveal what transition state geometry is favored in the absence of chiral auxiliary constraints. The lowest-energy transition structures **TS-2M** and **TS-2aP**, as well as a higher energy transition structure **TS-2bP**, are illustrated in Figure 2.

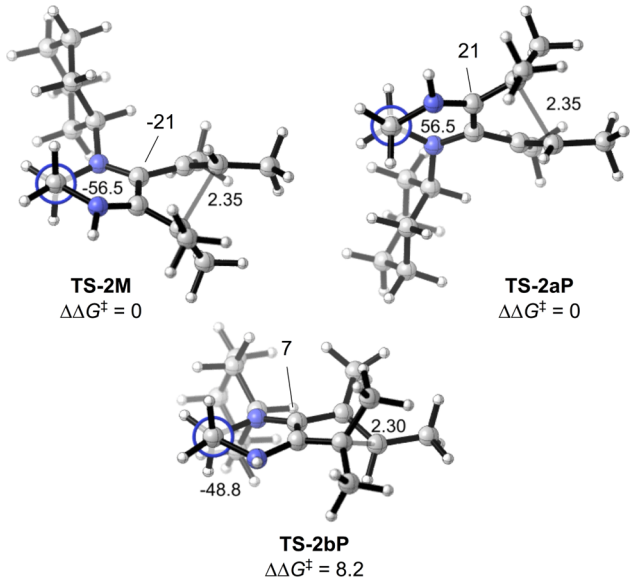

Figure 2. **TS-2M** and **TS-2aP** are the (enantiomeric) lowest-energy transition structures for the model Nazarov cyclization of the enamine−iminium intermediate derived from substrate **1** and diamine **II**. (M06-2X/def2-TZVPP−IEF-PCM//B3LYP/6-31G(d)−IEF-PCM (MeCN). **TS-2bP** is a higher energy transition structure similar to the geometry of **TS-1P**. The transition structures are illustrated as Newman projections through C6 and C7. The relative free energies of activation compared with **TS-2M** are reported in kcal/mol.

Figure 2 displays the Newman projections across C6 and C7 of the achiral diamine. **TS-2M** and **TS-2aP** are enantiomeric and isoenergetic in this model system. The dihedrals about C3 and C4 are −21° and 21°, respectively, due to the clockwise and counterclockwise twists of the cyclizing termini. In turn, this causes the N−C6−C7−N dihedral angles of **TS-2M** and **TS-2aP** to be −57° and 57°, respectively, in the half-chairs. **TS-2bP** is a higher-energy transition structure that leads to the minor (*R*)-product with a−49° N−C6−C7−N dihedral angle. **TS-2bP** is 8.2 kcal/mol higher in energy than **TS-2M**. The −49° dihedral forces the cyclization transition state to be nearly planar at C3−C4, resulting in the higher energy **TS-2aP**. The uncatalyzed parent Nazarov transition state (Figure S3) has a 31° dihedral at C3−C4, and locking the C6−C7 conformation into the (−)-gauche conformation favors the left-handed **M** helix of the cyclization transition state.

The transition structures (Figure 3) were calculated for the Nazarov cyclization of entry 2 (Scheme 1). In this case, the

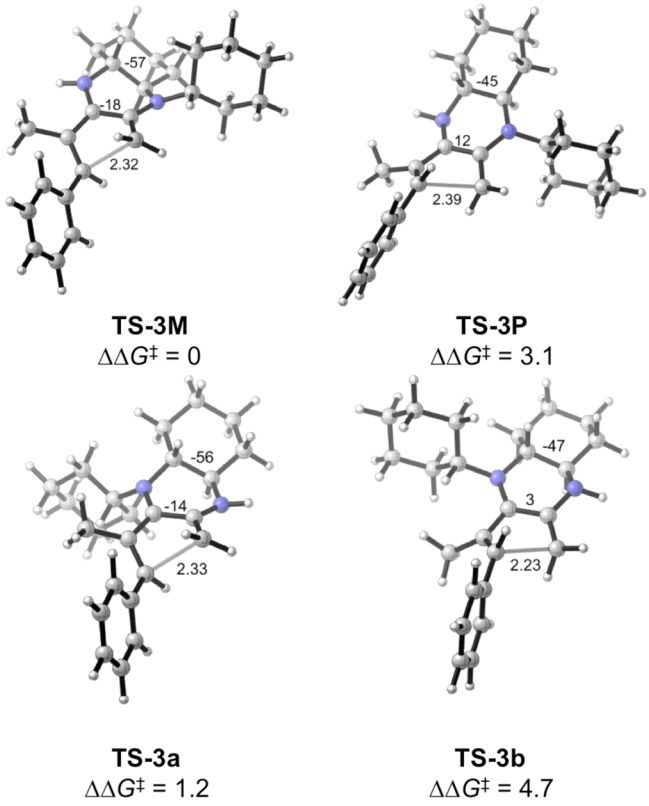

Figure 3. Lowest-energy transition structures for the Nazarov cyclization of the enamine−iminium intermediate for entry 2 in Scheme 1 leading to the major (*S*) and minor (*R*) products (M06-2X/def2-TZVPP−IEF-PCM//B3LYP/6-31G(d)−IEF-PCM (MeCN). The relative free energies of activation compared with **TS-3M** are reported in kcal/mol.

preferred enamine−iminium intermediate has a secondary nitrogen for the enamine and primary nitrogen for the iminium. However, this does not change the conformation of the amines, which are (−)-gauche. This preference is opposite of the enamine−iminium intermediate we calculated from entry 1. In this case, the enamine is unsubstituted. In entry 1, the enamine is substituted with methyl groups, which have closed-shell repulsions with the cyclohexyl ring. In each case, the difference in energy between the two arrangements in the electrocyclization transition state is less than 2 kcal/mol. The factors that control the stereoselectivity remain the same. The predicted difference in activation barrier ($\Delta\Delta G^{\ddagger}$) is 3.1 kcal/mol, which agrees closely with the experimentally observed enantioselectivity of 98.5% ($\Delta\Delta G^{\ddagger}$ = 2.9 kcal/mol).

■ CONCLUSIONS

The mechanism, source of product inhibition, and origins of stereoselectivity have been explained with density functional theory calculations. The reaction forms the enamine−iminium intermediate originally predicted by Tius.[6] The product inhibition occurs because the enamine−iminium cyclopente-

DOI: 10.1021/acs.joc.7b01606
J. Org. Chem. 2017, 82, 8186−8190

none-intermediate following cyclization is extremely stable and requires acidic conditions for hydrolysis to occur.

The diamine is locked into the (−)-gauche conformation, which favors left-handed helicity in the Nazarov transition state. The (−)-gauche diamine yields cyclizations with M helicity, and the (+)-gauche diamine is predicted to yield P helicity (Scheme 3). Torquoselectivity is achieved through the newly formed ring of the diamine and α-ketoenone. This six-membered ring favors one helical chirality of the cyclizing moiety of the Nazarov transition state. If product inhibition can be solved, this would provide another organocatalytic method for Nazarov cyclizations with high optical purity.

Scheme 3. Summary of Stereoselectivity Model

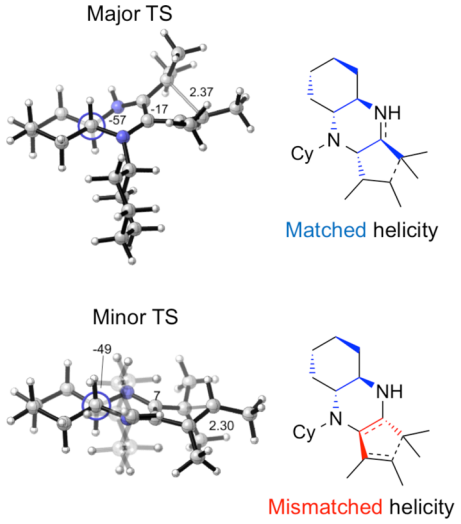

■ ASSOCIATED CONTENT

Supporting Information

The Supporting Information is available free of charge on the ACS Publications website at DOI: 10.1021/acs.joc.7b01606.

Complete set of intermediates, Nazarov cyclization transition structures, and their energies for the chiral vicinal diamine-mediated Nazarov reactions, Cartesian coordinates and thermodynamic parameters (in hartrees) of all stationary points (PDF)

■ AUTHOR INFORMATION

Corresponding Author

*E-mail: houk@chem.ucla.edu.

ORCID

Adam Simon: 0000-0001-6334-3359

Yu-hong Lam: 0000-0002-4946-1487

K. N. Houk: 0000-0002-8387-5261

Notes

The authors declare no competing financial interest.

■ ACKNOWLEDGMENTS

We thank Prof. Marcus Tius for discussions and helpful comments. Financial support is provided by the National Science Foundation (CHE-1361104). A.S. is a recipient of the NIH Chemistry-Biology Interface Research Training Grant (USPHS National Research Service Award T32GM008496). This work used computational and storage services associated with the Hoffman2 Shared Cluster provided by UCLA Institute for Digital Research and Education's (IDRE) Research Technology Group. The Extreme Science and Engineering Discovery Environment (XSEDE) was also used, which is supported by National Science Foundation grant number ACI-1053575.

■ REFERENCES

(1) (a) Nazarov, I. N.; Zaretskaya, I. I. *Izv. Akad. Nauk SSSR, Ser. Khim.* **1941**, 211−224. (b) Nazarov, I. N.; Zaretskaya, I. I. *Zh. Obshch. Khim.***1957**, *27*, 693−713.;. (c) Nazarov, I. N.; Zaretskaya, I. I.; Sorkina, T. I. *Zh. Obshch. Khim.* **1960**, *30*, 746−754.;. (c1) Shimada, N.; Stewart, C.; Tius, M. A. *Tetrahedron* **2011**, *67*, 5851−5870. (d) Tius, M. A. *Chem. Soc. Rev.* **2014**, *43*, 2979−3002. (e) West, F. G.; Scadeng, O.; Wu, Y.-K.; Fradette, R. J.; Joy, S. The Nazarov Cyclization. In *Comprehensive Organic Synthesis II*, 2nd ed.; Knochel, P., Molander, G. A., Eds.; Elsevier: The Netherlands, 2014; Vol. *5*, pp 827−866.

(2) (a) Liang, G.; Trauner, D. *J. Am. Chem. Soc.* **2004**, *126*, 9544−9545. (b) Liang, G.; Gradl, S. N.; Trauner, D. *Org. Lett.* **2003**, *5*, 4931−4934. (c) Nie, J.; Zhu, H.-W.; Cui, H.-F.; Hua, M.-Q.; Ma, J.-A. *Org. Lett.* **2007**, *9*, 3053−3056.

(3) (a) Pridgen, L. N.; Huang, K.; Shilcrat, S.; Tickner-Eldridge, A.; DeBrosse, C.; Halti-wanger, R. C. *Synlett* **1999**, *1999*, 1612−1614. (b) Kerr, D. J.; Metje, C.; Flynn, B. L. *Chem. Commun.* **2003**, *39*, 1380−1381. (c) Banaag, A. R.; Tius, M. A. *J. Org. Chem.* **2008**, *73*, 8133−8141. (d) Kerr, D. J.; White, J. M.; Flynn, B. L. *J. Org. Chem.* **2010**, *75*, 7073−7084. (e) Wu, Y.-K.; Niu, T.; West, F. G. *Chem. Commun.* **2012**, *48*, 9186−9188.

(4) (a) Rueping, M.; Ieawsuwan, W.; Antonchick, A. P.; Nachtsheim, B. J. *Angew. Chem., Int. Ed.* **2007**, *46*, 2097−2100. (b) Basak, A. K.; Shimada, N.; Bow, W. F.; Vicic, D. A.; Tius, M. A. *J. Am. Chem. Soc.* **2010**, *132*, 8266−8267. (c) Huang, Y.-W.; Frontier, A. J. *Tetrahedron Lett.* **2015**, *56*, 3523−3526.

(5) (a) Notz, W.; Tanaka, F.; Barbas, C. F., III. *Acc. Chem. Res.* **2004**, *37*, 580−591. (b) Trost, B. M.; Brindle, C. S. *Chem. Soc. Rev.* **2010**, *39*, 1600−1632.

(6) Bow, W. F.; Basak, A. K.; Jolit, A.; Vicic, D. A.; Tius, M. A. *Org. Lett.* **2010**, *12*, 440−443.

(7) (a) Smith, D. A.; Ulmer, C. W., II *Tetrahedron Lett.* **1991**, *32*, 725−728. (b) Shi, F.-Q.; Li, X.; Xia, Y.; Zhang, L.; Yu, Z.-X. *J. Am. Chem. Soc.* **2007**, *129*, 15503−15512. (c) Marcus, A. P.; Lee, A. S.; Davis, R. L.; Tantillo, D. J.; Sarpong, R. *Angew. Chem., Int. Ed.* **2008**, *47*, 6379−6383. (d) Lebœuf, D.; Huang, J.; Gandon, V.; Frontier, A. J. *Angew. Chem., Int. Ed.* **2011**, *50*, 10981−10985. (e) Kitamura, K.; Shimada, N.; Atesin, A. C.; Ateşin, T. A.; Tius, M. A.; Stewart, C. *Angew. Chem., Int. Ed.* **2015**, *54*, 6288−6291. (f) Lovie-Toon, J. P.; Tram, C. M.; Flynn, B. L.; Krenske, E. H. *ACS Catal.* **2017**, *7*, 3466−3476.

(8) Asari, A. H.; Lam, Y.-h.; Tius, M. A.; Houk, K. N. *J. Am. Chem. Soc.* **2015**, *137*, 13191−13199.

(9) Frisch, M. J.; Trucks, G. W.; Schlegel, H. B.; Scuseria, G. E.; Robb, M. A.; Cheeseman, J. R.; Scalmani, G.; Barone, V.; Mennucci, B.; Petersson, G. A.; Nakatsuji, H.; Caricato, M.; Li, X.; Hratchian, H. P.; Izmaylov, A. F.; Bloino, J.; Zheng, G.; Sonnenberg, J. L.; Hada, M.; Ehara, M.; Toyota, K.; Fukuda, R.; Hasegawa, J.; Ishida, M.; Nakajima, T.; Honda, Y.; Kitao, O.; Nakai, H.; Vreven, T.; Montgomery, J. A., Jr.; Peralta, J. E.; Ogliaro, F.; Bearpark, M.; Heyd, J. J.; Brothers, E.; Kudin, K. N.; Staroverov, V. N.; Keith, T.; Kobayashi, R.; Normand, J.; Raghavachari, K.; Rendell, A.; Burant, J. C.; Iyengar, S. S.; Tomasi, J.; Cossi, M.; Rega, N.; Millam, J. M.; Klene, M.; Knox, J. E.; Cross, J. B.; Bakken, V.; Adamo, C.; Jaramillo, J.; Gomperts, R.; Stratmann, R. E.; Yazyev, O.; Austin, A. J.; Cammi, R.; Pomelli, C.; Ochterski, J. W.; Martin, R. L.; Morokuma, K.; Zakrzewski, V. G.; Voth, G. A.; Salvador, P.; Dannenberg, J. J.; Dapprich, S.; Daniels, A. D.; Farkas, O.; Foresman, J. B.; Ortiz, J. V.; Cioslowski, J.; Fox, D. J. *Gaussian 09, Rev. D.01*; Gaussian, Inc.: Wallingford, CT, 2013.

DOI: 10.1021/acs.joc.7b01606
J. Org. Chem. 2017, 82, 8186−8190

(10) (a) Vosko, S. H.; Wilk, L.; Nusair, M. *Can. J. Phys.* **1980**, *58*, 1200−1211. (b) Lee, C.; Yang, W.; Parr, R. G. *Phys. Rev. B: Condens. Matter Mater. Phys.* **1988**, *37*, 785−789. (c) Becke, A. D. *J. Chem. Phys.* **1993**, *98*, 5648−5652. (d) Stephens, P. J.; Devlin, F. J.; Chabalowski, C. F.; Frisch, M. J. *J. Phys. Chem.* **1994**, *98*, 11623−11627.
(11) Tomasi, J.; Mennucci, B.; Cammi, R. *Chem. Rev.* **2005**, *105*, 2999−3094.
(12) (a) Ribeiro, R. F.; Marenich, A. V.; Cramer, C. J.; Truhlar, D. G. *J. Phys. Chem. B* **2011**, *115*, 14556−14562. (b) Zhao, Y.; Truhlar, D. G. *Phys. Chem. Chem. Phys.* **2008**, *10*, 2813−2818.
(13) Zhao, Y.; Truhlar, D. *Theor. Chem. Acc.* **2008**, *120*, 215−241.
(14) Weigend, F.; Ahlrichs, R. *Phys. Chem. Chem. Phys.* **2005**, *7*, 3297−3305.
(15) (a) Simoń, L.; Goodman, J. M. *Org. Biomol. Chem.* **2011**, *9*, 689−700. (b) Simon, A.; Lam, Y.-h.; Houk, K. N. *J. Am. Chem. Soc.* **2016**, *138*, 503−506. (c) Lam, Y.-h.; Grayson, M. N.; Holland, M. C.; Simon, A.; Houk, K. N. *Acc. Chem. Res.* **2016**, *49*, 750−762.

DOI: 10.1021/acs.joc.7b01606
J. Org. Chem. 2017, 82, 8186−8190